

Systematics of carbon + carbon fusion-evaporation reactions

B. Heusch, C. Beck, J. P. Coffin, R. M. Freeman, A. Gallmann, F. Haas, F. Rami, P. Wagner, and D. E. Alburger*

Centre de Recherches Nucléaires et Université Louis Pasteur, 67037 Strasbourg Cedex, France

(Received 8 September 1980)

Carbon + carbon fusion-evaporation reactions have been studied in two series of measurements: (i) The system $^{13}\text{C} + ^{13}\text{C}$ has been studied for laboratory bombarding energies between 30 and 60 MeV in 5-MeV steps. Angular distributions for all residual nuclei have been measured and the corresponding yields versus bombarding energy are compared to a fusion-evaporation calculation. It is also shown that, at least at one bombarding energy, the fusion evaporation residue yields for the $^{12}\text{C} + ^{14}\text{C}$ and $^{13}\text{C} + ^{13}\text{C}$ systems are almost the same, confirming the independence of the way in which the compound nucleus ^{26}Mg is formed. (ii) The systems $^{12}\text{C} + ^{12}\text{C}$, $^{13}\text{C} + ^{12}\text{C}$, $^{13}\text{C} + ^{13}\text{C}$, and $^{13}\text{C} + ^{14}\text{C}$ have been studied at $E_{\text{lab}} = 40$ MeV. This energy corresponds approximately to the maxima of the fusion evaporation cross sections for all these systems. The yields to final residual nuclei show that the additional neutrons strongly affect mainly the αxn and $2\alpha xn$ channels and this is well reproduced by the Hauser-Feshbach statistical model. The results are compared to those obtained for neighboring fusion-evaporation systems.

NUCLEAR REACTIONS ^{12}C and ^{13}C beams on ^{12}C , ^{13}C , and ^{14}C targets; natural and enriched targets; $30 \leq E$ (lab) ≤ 60 MeV; time of flight with Z identification technique; fusion-evaporation yields; comparison with statistical particle evaporation calculations.

I. INTRODUCTION

Many experimental and theoretical studies have been devoted to the complete fusion of heavy ions,^{1,2} with two main fields of interest: the saturation of the fusion corresponding to the concept of a critical radius, and the resonance phenomena observed essentially for the α -like nuclear systems such as $^{12}\text{C} + ^{12}\text{C}$, $^{12}\text{C} + ^{16}\text{O}$, and $^{16}\text{O} + ^{16}\text{O}$.³ For such systems it has been shown that gross and intermediate structures are observed as much for fusion evaporation (mainly α channels) as for direct channels. However, the influence of an additional valence neutron to such α -like systems seems to wash out these oscillations from the fusion channels, whereas they remain in the direct channels.⁴ In this context it was interesting to make systematic studies of the carbon + carbon systems by analyzing first the decay of a "non-resonating" system ($^{13}\text{C} + ^{13}\text{C}$) over the "plateau" of the total fusion-evaporation cross section⁴ and, second, by looking at the influence on these cross sections of the addition of up to three neutrons to the $^{12}\text{C} + ^{12}\text{C}$ system at an incident energy $E_{\text{c.m.}} = 20$ MeV. This value near twice the Coulomb barrier corresponds approximately to the maximum of all total fusion-evaporation cross sections.³

Mass and Z identification have been achieved for each evaporation residue. Such a detailed study has never been done for such very light systems; only isotope-integrated cross sections have been reported for $^{12}\text{C} + ^{12}\text{C}$ (Refs. 3 and 5) and $^{12}\text{C} + ^{13}\text{C}$.³ However, precise excitation functions

have been obtained in our laboratory, by the use of γ techniques, for $^{12}\text{C} + ^{12}\text{C}$,⁶ $^{12}\text{C} + ^{13}\text{C}$,⁴ and $^{14}\text{C} + ^{12}\text{C}$.⁷ Knowing the advantages and disadvantages of each technique, the present experiments appear as complementary to our γ studies in the sense that only the total residue formation yields presented here can be compared in detail to evaporation calculations.

The "statistical" aspect of the compound nucleus deexcitations has been checked by measuring the influence on the evaporation residue yields of changes in the bombarding energy (and hence angular momentum dissipated) and of changes in the neutron excess of the compound system. In each case, a detailed comparison with the statistical model of Hauser-Feshbach has been carried out.

II. EXPERIMENTAL PROCEDURE.

Beams of ^{12}C and ^{13}C were obtained from the Strasbourg MP tandem accelerator. Self-supporting ^{12}C and ^{13}C targets of $80 \mu\text{g}/\text{cm}^2$ were used; the ^{13}C targets were 98.5% isotopically enriched. The ^{14}C target obtained from the University of Munich was $100 \mu\text{g}/\text{cm}^2$ thick, 80% isotopically enriched. From the present elastic scattering cross section measurements, the ^{12}C contamination was found to be 23.8%.

The mass identification was obtained from a time of flight system already described elsewhere.^{8,9} The start detector consisted of a carbon foil-channel plate assembly, and the stop signal was given by a solid state detector (300 μm thick

with a 450 mm² surface) located at 150 cm from the start detector. A time resolution of 200 ps [full width at half maximum (FWHM)] was obtained, corresponding to a total separation of each mass. In Fig. 1 typical spectra measured for all systems at $E_{\text{lab}} = 40$ MeV and $\theta_{\text{lab}} = 10^\circ$ are presented. The Z identification was achieved by an ionization chamber 10 cm long, operating with a 90% Ar, 10% CH₄ gas mixture at a pressure of 15 Torr. In Fig. 2 typical spectra measured for the reaction $^{13}\text{C} + ^{13}\text{C}$ at $E_{\text{lab}} = 60$ MeV are presented. Two monitors, located at $\pm 11^\circ$, near the target, and out of the time of flight-beam plane, were used for normalization purposes.

Angular distributions were measured at least at five angles ($\theta_{\text{lab}} = 5^\circ, 10^\circ, 15^\circ, 20^\circ,$ and 25°) for all systems and energies. The normalizations have been achieved using either the Rutherford scattering or an optical model calculation (code GENOVA¹⁰). However, a difficulty of these simultaneous mass and Z measurements is related to the angular straggling in the start foil, which is, for low heavy-ion recoil velocities, larger than for the elastic scattered carbon ions. In Fig. 3

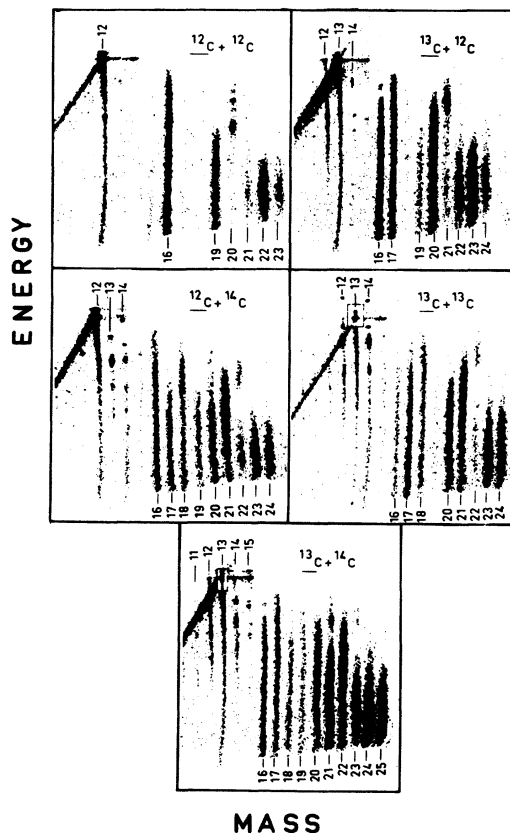


FIG. 1. Two-dimensional energy versus mass spectra measured for each indicated reaction at $E_{\text{lab}} = 40$ MeV and $\theta_{\text{lab}} = 10^\circ$. The underlined ion is the projectile.

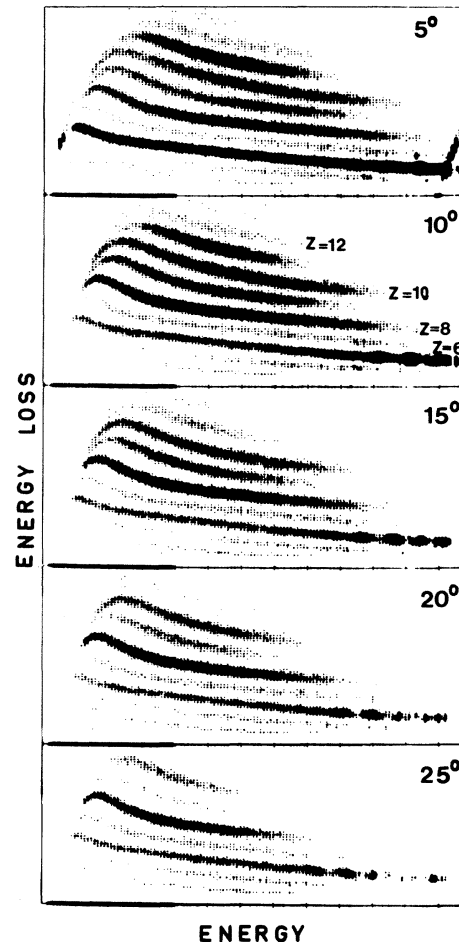


FIG. 2. Two-dimensional energy-loss versus energy spectra measured with the ionization chamber for the reaction $^{13}\text{C} + ^{13}\text{C}$ at $E_{\text{lab}} = 60$ MeV. The angular distribution has been measured at the five indicated laboratory angles.

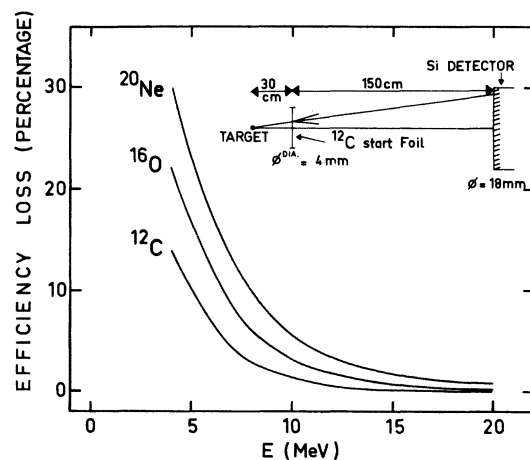


FIG. 3. Calculated efficiency loss percentages, for three recoiling heavy fragments, versus their energy, due to the angular straggling in the start foil. The geometrical experimental conditions are indicated.

the results of such a calculation using the collision theory of Meyer¹¹ are illustrated. It can be seen that for recoil velocities less than 7 MeV, and down to the 4 MeV threshold, this effect can be large. Corrections to the data for this straggling effect, which become important for beam energies $E_{\text{lab}} \leq 40$ MeV, along with the energy threshold effects, have not been carried out. Such corrections could be possible but, beside the fact that they are ion mass and energy dependent, they are also affected by stopping power and foil thickness uncertainties, leading to too large uncertainties in the absolute fusion-evaporation residue cross-section values at low energies. Therefore we report only relative cross sections which are sufficient for the purpose of the present studies. For these values, although the error due to straggling is greater for the heavier ions, there is a compensating effect, as the energies are also greater. It is difficult to correctly estimate quantitatively these effects on the relative yields, but we did have an additional check, the calculated angular distributions using the code LILITA.¹² In the extreme case we estimate that there could be additional uncertainties up to $\pm 5\%$ for bombarding energies below 40 MeV. It should be noticed that our yields are in very good agreement with those extracted for $^{12}\text{C} + ^{12}\text{C}$ at $E_{\text{c.m.}} = 20$ MeV by Kovar *et al.*³ and Conjeaud *et al.*,⁵ and for $^{13}\text{C} + ^{12}\text{C}$ by Kovar *et al.*³

III. EXPERIMENTAL RESULTS

In order to emphasize the most striking behavior of the measured yields, we will present our results by considering first, for each Z number, the sum over the corresponding isotopes, which is directly comparable to other published results. Then, going into greater detail, the individual residue feedings will be presented. All measured yields have $\pm 5\%$ errors, which are composed of $\pm 1-3\%$ statistical uncertainties and $\pm 3-5\%$ errors in the estimation of the integral of the angular distributions. For the angles beyond $25^\circ-30^\circ$ only the $2\alpha xn$, and to a lesser extent αxn , channels have non-negligible contributions. The value at 30° was obtained by linear extrapolation of the values at 20° and 25° , assuming zero at 35° , whereas for $^{12}\text{C} + ^{12}\text{C}$ and $^{12}\text{C} + ^{14}\text{C}$ we measured out to 30° . We confirmed that the curve so obtained followed the form calculated by the code LILITA.¹² From this we estimated a $\pm 5\%$ error, whereas the statistical error was only about $\pm 1\%$.

A. The $^{13}\text{C} + ^{13}\text{C}$ reaction

In Fig. 4 the experimental results are presented on the left-hand side, along with the theoretical

predictions (discussed in the next section) on the right-hand side. The system $^{13}\text{C} + ^{13}\text{C}$ has been studied between 30 and 60 MeV bombarding energy in 5 MeV steps. The trend of all excitation functions is that they are nearly all monotonic with two dominant features: (i) the Ne and O isotope yields have very strong, but exactly opposite, evolutions within the bombarding energy range, decreasing for Ne, for instance, from 50% down to 20% of the total fusion evaporation cross section; (ii) all other channels display less sensitivity to the energy. However, the same tendency is observed as for the αxn and $2\alpha xn$ channels, that is, the higher the energy, the greater the number of particles which must be evaporated to reduce the temperature of the compound nucleus. For example, the $p xn$ channels (leading to Na isotopes) have an opposite trend to the $\alpha p xn$ ones (leading to F isotopes) with increasing energies. In Fig. 5 all the corresponding individual isotope yields along with the theoretical predictions (see next section) are shown. As is illustrated in an inset of Fig. 5, one observes over the whole energy range a constant total feeding of all oxygen and neon isotopes with a mean value of $(66.6 \pm 1.8)\%$ of $\sigma_{\text{F.E.}}$ (the total fusion-evaporation cross section); at low energies the αxn (mainly αn to ^{21}Ne) can remove enough angular momentum, whereas at high energy the $2\alpha xn$ ($2\alpha n$ to ^{17}O and $2\alpha 2n$ to ^{16}O ; see Fig. 5) evaporations are necessary. In the case of $^{12}\text{C} + ^{12}\text{C}$, only the 2α channel to ^{16}O dominates over the same energy range (see Fig. 4 of Ref. 3), whereas for $^{14}\text{N} + ^{12}\text{C}$ (forming the isobar compound nucleus ^{26}Al) and $^{15}\text{N} + ^{12}\text{C}$ (Fig. 11 of Ref. 3) all cross sections are nearly

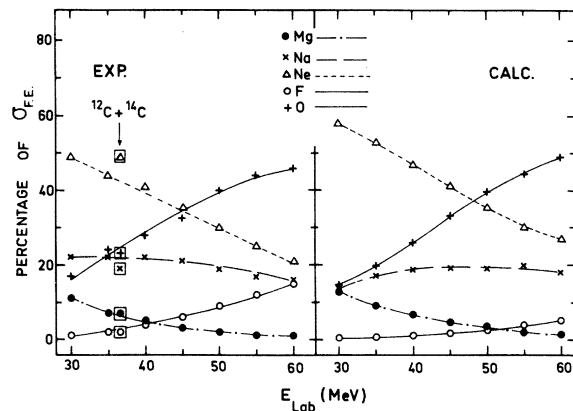


FIG. 4. Experimental and calculated relative element fusion evaporation yields versus bombarding energy for the $^{13}\text{C} + ^{13}\text{C}$ reaction. The corresponding results for the ^{12}C on ^{14}C study are indicated inside the squares. Relative errors of $\pm 5\%$ on the experimental values are not shown. The calculated values are obtained using the code LILITA.

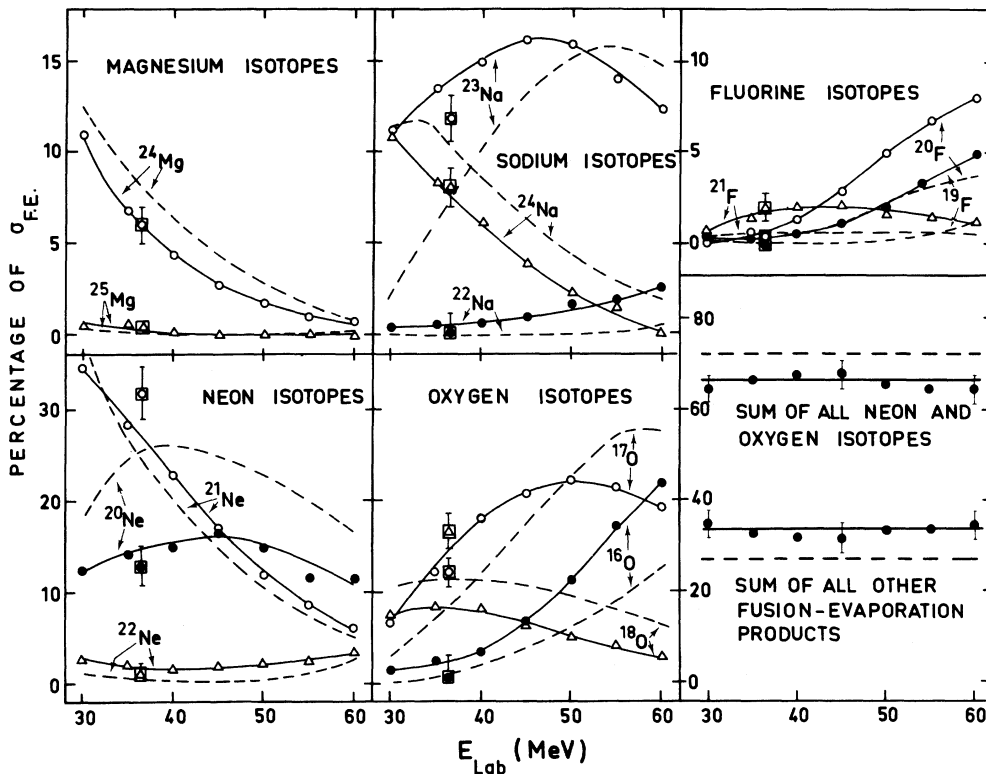


FIG. 5. Experimental individual isotopes relative cross sections (full lines) versus bombarding energy for the $^{13}\text{C} + ^{13}\text{C}$ reaction. Relative errors of $\pm 5\%$ are not shown. The dotted lines give the predictions of the evaporation code LILITA. Experimental results for $^{12}\text{C} + ^{14}\text{C}$ are indicated inside the squares.

constant, varying within less than 10% of $\sigma_{\text{F.E.}}$, for $15 \leq E_{\text{c.m.}} \leq 26$ MeV.

The cross sections for the $^{13}\text{C} + ^{13}\text{C}$ direct channels have also been obtained and are given in Fig. 6. Here, neither the energy threshold nor the straggling effect influence the results, since these channels correspond to much higher recoil velocities than for evaporation residues. Therefore we report absolute cross-section values corresponding to the measured angular range ($\theta_{\text{lab}} \leq 30^\circ$). By "inelastic" we refer to the cross sections corresponding to the excitation of the three bound levels of ^{13}C at 3.09, 3.65, and 3.85 MeV. The same sum is obtained for the mutual excitation of the beam and the target ^{13}C ions. The cross sections for the transfer channels are dominated strongly (near 90%) by the one-neutron transfer to $^{12}\text{C} + ^{14}\text{C}$ over the whole energy range; the other main channels are $^{11}\text{B} + ^{15}\text{N}$ (about 4%) and $^9\text{Be} + ^{17}\text{O}$ (~3%).

B. The C+C systems

The experimental results obtained for the system $^{12}\text{C} + ^{14}\text{C}$, which leads to the same compound nucleus (^{26}Mg), as $^{13}\text{C} + ^{13}\text{C}$, are also plotted in

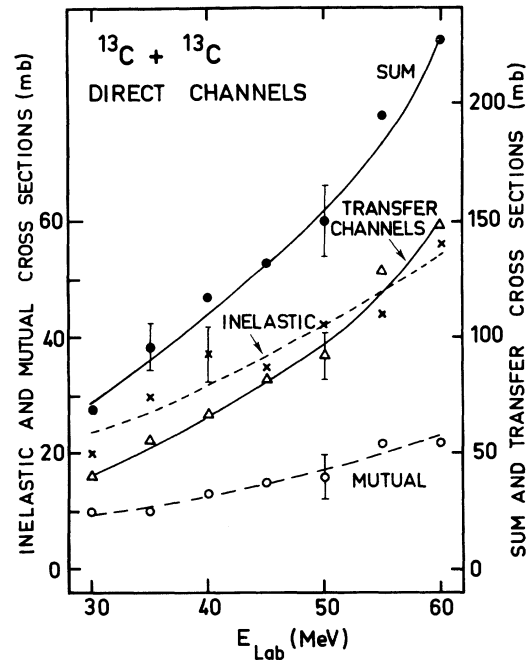


FIG. 6. Direct channel absolute cross sections measured for the reaction $^{13}\text{C} + ^{13}\text{C}$, versus bombarding energy, in the angular range $\theta_{\text{lab}} \leq 30^\circ$.

Figs. 4 and 5. This study, done at $E_{\text{lab}}(^{12}\text{C}) = 40$ MeV, corresponds exactly to the same excitation energy in ^{26}Mg ($E = 40.77$ MeV) as the system $^{13}\text{C} + ^{13}\text{C}$ at $E_{\text{lab}}(^{13}\text{C}) = 36.62$ MeV. The important amount of ^{12}C in the ^{14}C target could be correctly estimated using the elastic scattering data of the ^{12}C beam on ^{12}C and ^{14}C , which were well separated for $\theta_{\text{lab}} \geq 15^\circ$. The contribution of the $^{12}\text{C} + ^{12}\text{C}$ evaporation residue cross sections have been subtracted by appropriate normalization to the $^{12}\text{C} + ^{12}\text{C}$ study at $E_{\text{lab}} = 40$ MeV. Though the errors are larger for $^{12}\text{C} + ^{14}\text{C}$ (10% versus 5% for $^{13}\text{C} + ^{13}\text{C}$), we can say that good agreement is found for the two entrance channels, except for ^{18}O ; this will be discussed later.

All C + C systems have been studied at the same bombarding energy, $E_{\text{lab}} = 40$ MeV. In Fig. 7 the results, together with the corresponding predictions are presented. For the $^{13}\text{C} + ^{14}\text{C}$ system, the contribution of ^{12}C in the ^{14}C target must also be subtracted in the same way as for $^{12}\text{C} + ^{14}\text{C}$. The lines drawn between the different points have, of course, no physical meaning but, guiding the eye, they illustrate the trends of the results which follow: (i) the neon and oxygen isotopes, which correspond to αxn and $2\alpha xn$ deexcitation channels, dominate strongly, always taking more than 60% of $\sigma_{\text{F.E.}}$; the oxygen feeding decreases very rapidly with the increase of the neutron number, whereas the neon has nearly exactly the opposite trend; (ii) the other deexcitation channels have a quite smooth variation from one system to another, except for the $^{13}\text{C} + ^{14}\text{C}$ system, where a strong feeding of the Mg isotopes is observed, corresponding essentially to the evaporation of 2 and 3 neutrons.

For the two dominant fusion-evaporation residue

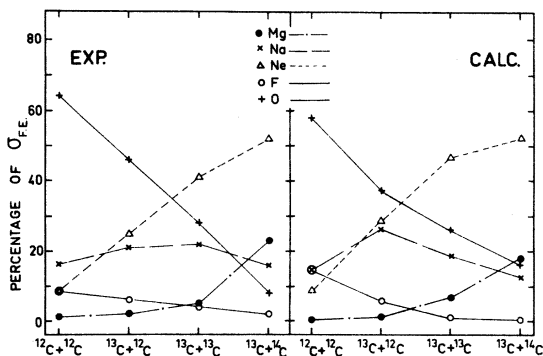


FIG. 7. Experimental and calculated relative element fusion evaporation yields for all indicated C + C systems, at $E_{\text{lab}} = 40$ MeV, the first indicated nucleus being the projectile. Lines between all points are only a guide to the eye. Relative errors of $\pm 5\%$ on the experimental values are not shown.

formations for all C + C systems, the individual isotope feedings are reported in Fig. 8. This figure illustrates the drastic change in these α emission channels. For example, for $^{12}\text{C} + ^{12}\text{C}$, the feeding of ^{16}O corresponds to 60% of the fusion-evaporation process, whereas for $^{13}\text{C} + ^{14}\text{C}$, no individual isotope of oxygen accounts for more than 4% of $\sigma_{\text{F.E.}}$. The differences between the residue distributions observed for $^{12}\text{C} + ^{12}\text{C}$ up to $^{13}\text{C} + ^{14}\text{C}$ are due to a continuous increase of the tendency to return to the β -stability line when the number of neutrons increases. The differences in the magnitudes of the different deexcitation channels are also related to the possibility, for neutron-rich systems to dissipate enough angular momentum by $p xn$ and αxn channels, whereas for $^{12}\text{C} + ^{12}\text{C}$ only the 2α channel can do this.

IV. DISCUSSION

All calculated cross sections reported in Figs. 4, 5, 7, and 8 have been obtained by using the code LILITA,¹² which evaluates the predictions of the Hauser-Feshbach statistical model by a Monte Carlo method. In these calculations all parameters have been taken as in our preceding $^{16}\text{O} + ^{12}\text{C}$ (Ref. 13) and $^{16}\text{O} + ^{16}\text{O}$ (Ref. 14) studies; the sensitivity to the particular chosen parameters for level densities and transmission coefficients has been discussed in Ref. 13. The critical angular momenta l_{cr} introduced in the present calculations

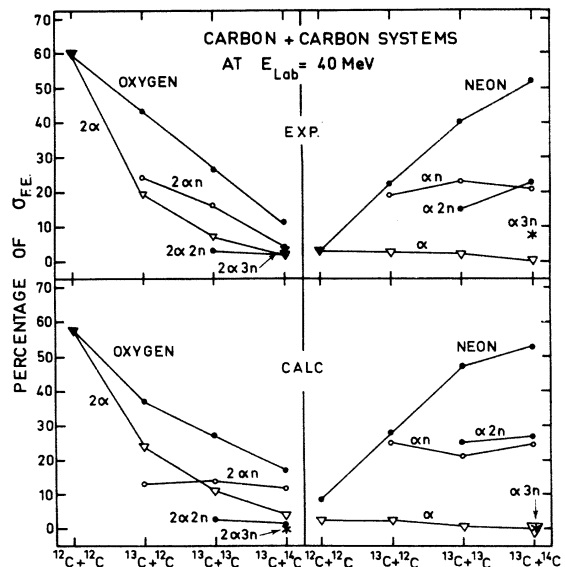


FIG. 8. Experimental and calculated (LILITA code results) oxygen and neon individual isotope yields for all C + C systems at $E_{\text{lab}} = 40$ MeV. Lines are only a guide to the eye.

are listed in Table I. These values are obtained using the sharp cutoff approximation, either from experimental absolute cross section measurements or by extrapolating them from the latter using a $\Delta l = +0.5\hbar$ criterion for one additional neutron. However, in contrast to the absolute total fusion cross sections, the relative yields reported in Figs. 4, 5, 7, and 8 are rather insensitive to a small change in the value of l_{cr} . For example, for the $^{13}\text{C} + ^{13}\text{C}$ system at $E_{c.m.} = 20$ MeV, we took $l_{cr} = 13\hbar$ (corresponding to $\sigma_{F.E.} = 990$ mb); a $\Delta l_c = \pm 0.5\hbar$ gives maximum deviations of 0.5% for Mg, Ne, and F isotopes, and 1.0% for Na and O for the calculated relative yields (Fig. 4), whereas it corresponds to $\Delta\sigma_{F.E.} = \pm 70$ mb (7% effect). From an overall comparison between experimental and calculated isotope yields, two main conclusions can be drawn: (i) generally good agreement is found between the predictions of LLLITA and all element distributions measured either for $^{13}\text{C} + ^{13}\text{C}$ versus bombarding energy (Fig. 4), or for the C+C systems at $E_{lab} = 40$ MeV (Fig. 7). (ii) The individual isotope predictions (Figs. 5 and 8) are, however, worse in magnitude and, moreover, in some cases a shift of the calculated curve is observed; we verified that this cannot be attributed to a critical angular momentum choice problem. In respect to the approximations made in the LLLITA code, especially for the level densities, it does not seem worthwhile to

TABLE I. Critical angular momenta introduced in the evaporation calculations.

Reaction	$E_{c.m.}$ (MeV)	l_{cr} (\hbar)
$^{13}\text{C} + ^{13}\text{C}$	15.0	10.5
	17.5	12.0
	20.0	13.0 ^a
	22.5	13.5
	25.0	14.5
	27.5	15.0
$^{12}\text{C} + ^{12}\text{C}$	30.0	15.5
	20.0	12.0 ^b
$^{13}\text{C} + ^{12}\text{C}$	19.2	12.5 ^c
$^{13}\text{C} + ^{14}\text{C}$	20.7	13.5

^aValue taken by analogy to $^{12}\text{C} + ^{14}\text{N}$ at $E_{c.m.} = 20$ MeV from Kovar *et al.* (Ref. 3) and Conjeaud *et al.* (Ref. 5); $l_{cr} = (13 \pm 0.3)\hbar$.

^bMean value extracted from Kovar *et al.* (Ref. 3); $\sigma_{F.E.} = 906$ mb at $E_{c.m.} = 19.97$ and Conjeaud *et al.* (Ref. 5); $\sigma = 936$ mb at $E_{c.m.} = 20.0$ MeV.

^cKovar *et al.* (Ref. 3) report $\sigma_{F.E.} = 944$ mb at $E_{c.m.} = 19.14$ MeV, which corresponds to $l_{cr} = 12.1\hbar$.

adjust the corresponding parameters to obtain a better individual isotope fit, especially since they have been optimized for the neighboring system $^{12}\text{C} + ^{14}\text{N}$. We also ran the fusion-evaporation code CASCADE from Pühlhofer.¹⁵ In this case we used the whole set of parameters used by Pühlhofer¹⁵ for $^{19}\text{F} + ^{12}\text{C}$ with the critical angular momenta

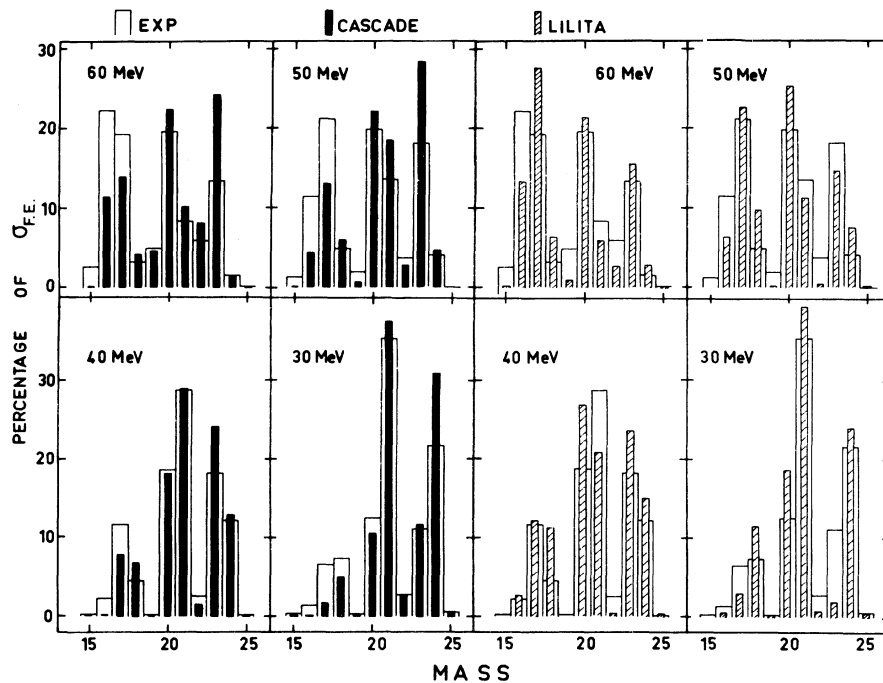


FIG. 9. comparison between experimental mass distributions obtained for $^{13}\text{C} + ^{13}\text{C}$ at four laboratory bombarding energies and the calculated ones using either the code CASCADE (left hand side) or LILITA (right hand side).

given in Table I. The major difference between the two codes is that the discrete energy levels are not considered in LILITA, whereas in CASCADE the experimental energy levels up to 7.5 MeV excitation energy are introduced into the calculation. CASCADE should therefore be more realistic, though both codes give good results, isotope by isotope, for $^{12}\text{C} + ^{12}\text{C}$. The good results for LILITA can be judged in Figs. 7 and 8, and for CASCADE see Conjeaud *et al.*⁵ But for $^{12}\text{C} + ^{12}\text{C}$, the results are relatively simple, with only one isotope appreciably populated for each Z , in general. For the other systems, a wider range of isotopes is formed. In Fig. 9 the results of the calculations for the $^{13}\text{C} + ^{13}\text{C}$ fusion-evaporation mass distributions are presented along with the data. The comparison of the LILITA and with CASCADE calculations to the data (Fig. 9) shows essentially that both codes give reasonable overall predictions but that, for the $^{13}\text{C} + ^{13}\text{C}$ system, precise individual isotope fits are difficult to obtain. As is illustrated in Fig. 8, except for $^{12}\text{C} + ^{12}\text{C}$, this is a general trend in all neutron-rich carbon systems, and is also observed for the neutron-rich $^{18}\text{O} + ^{12}\text{C}$ system we studied recently.¹⁷ However, for systems where the compound nucleus is close to the stability line [$^{12}\text{C} + ^{12}\text{C}$, $^{14}\text{N} + ^{12}\text{C}$, $^{12}\text{ }^{19}\text{F} + ^{12}\text{C}$, $^{15,16}\text{ }^{16}\text{O} + ^{12}\text{C}$ (Ref. 18)] the element and the individual isotope yields are well predicted. These calculations depend on a detailed knowledge of the yrast lines of the intermediate nuclei; this information is not so well known for neutron-rich nuclei, and this may be the origin for the differences we have noted with experiment.

It is often suggested that precompound particle emission occurs, which could also explain these observed discrepancies between data and evaporation calculations, as has been shown for the $^{19}\text{F} + ^{12}\text{C}$ system at a higher energy.¹⁶ If such a mechanism were important, it could result in detectable differences between the isotope production cross sections for the two systems $^{13}\text{C} + ^{13}\text{C}$ and $^{12}\text{C} + ^{14}\text{C}$, as the valence neutron is bound by only 4.9 MeV in ^{13}C , whereas for the second system it is the α particle of ^{12}C which is the least bound. In general, we have not observed any differences between the two systems, at least for energies around $E_{\text{lab}} = 40$ MeV. The only significant discrepancy is for ^{18}O , which is not formed by the emission of neutrons. This agrees with a similar conclusion we were able to draw recently by comparing the $^{18}\text{O} + ^{12}\text{C}$ and $^{16}\text{O} + ^{14}\text{C}$ systems.¹⁷

For the direct channels we present the different contributions for the $^{13}\text{C} + ^{13}\text{C}$ system in Fig. 6. For the other systems where target and projectile nuclei are not identical, the separation between transfer and inelastic is not possible. In Fig. 10,

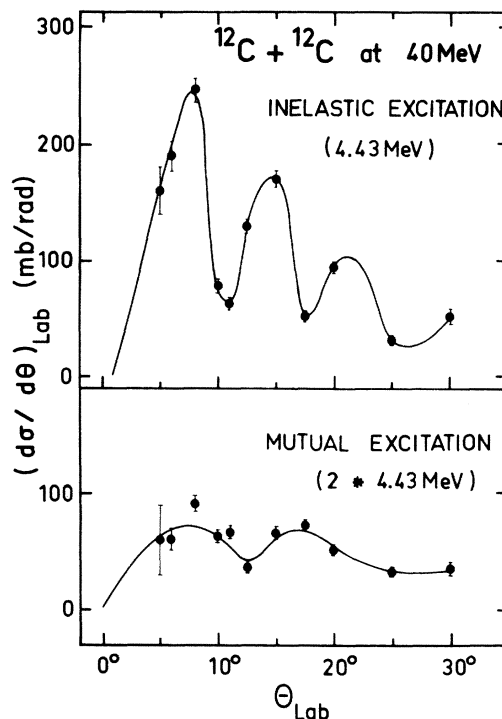


FIG. 10. Angular distributions of the inelastic and mutual excitation of the ^{12}C nuclei measured for the $^{12}\text{C} + ^{12}\text{C}$ reaction at $E_{\text{lab}} = 40$ MeV. Lines have been drawn for integration purpose for $\theta_{\text{lab}} \leq 30^\circ$.

for $^{12}\text{C} + ^{12}\text{C}$, the only direct channels observed at 40 MeV, which are the inelastic and mutual excitations are plotted; by integrating these angular distributions over the measured angular range we obtained 55 and 29 mb, respectively. These values are in good agreement with those obtained by Cormier *et al.*¹⁹ (84 and 44 mb, re-are smaller by a factor $\approx \frac{2}{3}$ since we included measurements only up to $\theta_{\text{c.m.}} = 60^\circ$, rather than to 90°). The comparison of our total direct cross section (84 ± 10 mb) for $^{12}\text{C} + ^{12}\text{C}$ at $E_{\text{c.m.}} = 20$ MeV to the corresponding value for $^{13}\text{C} + ^{13}\text{C}$ (120 ± 15 mb) illustrates the growing importance of the direct channels with the increasing number of neutrons. This is essentially due to the transfer channels such as $^{12}\text{C} + ^{14}\text{C}$ for the $^{13}\text{C} + ^{13}\text{C}$ reaction.

In this context it is interesting to look at very recent calculations by Abe and Haas,²⁰ who count the number of all open channels available per unit of flux versus the grazing angular momentum for all possible binary products, which include the compound and direct reaction channels. In Fig. 11 the corresponding results for all C+C systems we studied are plotted. The rise at high energies is due to the increasing importance of the direct channels, which are more capable of removing the highest angular momenta introduced in the

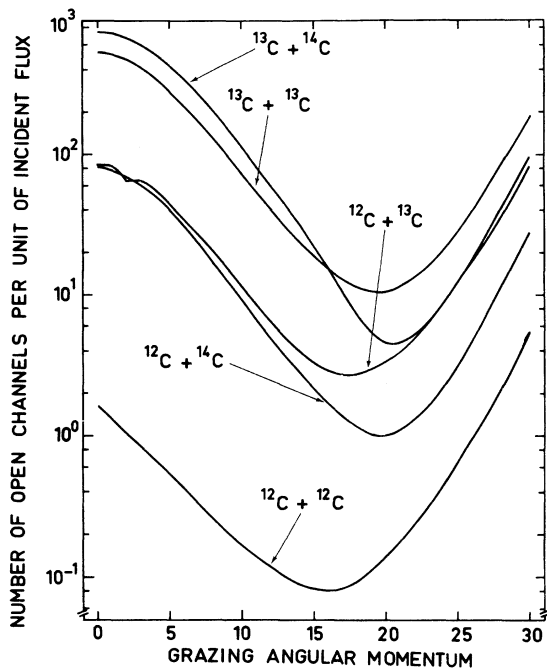


FIG. 11. Number of open channels per unit of flux versus grazing angular momentum calculated, for all C+C systems, by Abe and Haas (Ref. 20).

entrance channel. This is illustrated in Fig. 6 for $^{13}\text{C} + ^{13}\text{C}$ by the increase of the total direct cross section with bombarding energy. There are fewer competing open channels for the $^{12}\text{C} + ^{14}\text{C}$ system, and consequently the direct reactions should be stronger. In particular, if the α transfer is stronger in $^{12}\text{C} + ^{14}\text{C}$, this would explain the discrepancy in the ^{18}O production between the two systems which was noted above and has also been observed in γ measurements.⁴ The enhancement of the α transfer cross section, which could also be due to the intrinsic α structure of the ^{12}C nucleus as well as the number of open channels, has also been observed in the $^{16}\text{O} + ^{14}\text{C}$ reaction.²¹

V. CONCLUSION

We present in this work a complete identification in mass and atomic number for the fusion evapora-

tion residues formed by the reaction ^{13}C on ^{13}C between 15 and 30 MeV center-of-mass energies. The corresponding relative yields show that, although the neutron and (or) proton deexcitation channels vary little over the considered energy range, the αxn and $2\alpha xn$ yields vary drastically with opposite trends: the αxn channels drop with increasing energy, whereas the $2\alpha xn$ channels are increasing, corresponding to the necessity of removing greater excitation energy and greater angular momentum. For all carbon + carbon fusion-evaporation systems also studied at $E_{\text{lab}} = 40$ MeV, these general observations remain, but this time with a large increase of the αxn channels (and a large decrease of $2\alpha xn$ ones) with larger neutron numbers. This corresponds essentially to a tendency to return to the β -stability line for the heaviest Mg compound isotopes. All of these trends, generally considered characteristic of evaporation reactions, are less apparent in neighboring systems such as $^{12}\text{C} + ^{12}\text{C}$, $^{12}\text{C} + ^{14}\text{N}$, or $^{12}\text{C} + ^{15}\text{N}$, for example; this is interpreted as due to Q -value effects.

Evaporation calculations have shown that an overall satisfactory agreement is found for all C+C systems we studied either versus the bombarding energy or versus the neutron number only as far as the element distributions are concerned. As in the $^{18}\text{O} + ^{12}\text{C}$ reaction, we can conclude that the differences between such calculations and the data for individual isotopes cannot be attributed to incomplete fusion processes at the considered bombarding energies. The present systematic studies suggest that the failures of compound nucleus deexcitation calculations are mainly related to the estimation of the yrast line in neutron-rich nuclei.

Besides the statistical aspect of the compound nucleus deexcitation, we have shown the growing importance, between $^{12}\text{C} + ^{12}\text{C}$ and $^{13}\text{C} + ^{13}\text{C}$, of all direct channels. A calculation of all open channels capable of removing the angular momentum introduced in the entrance channel shows that their number can be very different from one system to another, explaining therefore a different partition of the total reaction cross section.

*Permanent address: Brookhaven National Laboratory, Upton, New York.

¹See, for instance, review articles such as J. R. Birkenlund, L. E. Tubbs, J. R. Huizenga, J. N. De, and D. Sperber, Phys. Rep. **56**, 107 (1979).

²D. Glas and U. Mosel, Phys. Rev. C **10**, 2620 (1974); Nucl. Phys. **A237**, 429 (1975).

³D. G. Kovar, D. F. Geesaman, T. H. Braid, Y. Eisen,

W. Henning, T. R. Ophel, M. Paul, K. E. Rehm, S. J. Sanders, P. Sperr, J. P. Schiffer, S. L. Tabor, S. Vigdor, and B. Zeidmann, Phys. Rev. C **20**, 1305 (1979).

⁴F. Haas, C. Beck, R. M. Freeman, A. Gallmann, and B. Heusch (unpublished); C. Beck, thesis, Strasbourg, Report No. CRN/PN 80-08, 1980 (unpublished).

⁵M. Conjeaud, S. Gary, S. Harar, and J. P. Wieleczko,

- Nucl. Phys. A309, 515 (1978).
- ⁶J. J. Kolata, R. M. Freeman, F. Haas, B. Heusch, and A. Gallmann, Phys. Rev. C 21, 579 (1980).
- ⁷R. M. Freeman, F. Haas, and G. Korschinek, Phys. Lett. 90B, 229 (1980).
- ⁸J. P. Coffin, P. Engelstein, A. Gallmann, B. Heusch, P. Wagner, and H. E. Wegner, Phys. Rev. C 17, 1607 (1978).
- ⁹H. Oeschler, P. Wagner, J. P. Coffin, P. Engelstein, and B. Heusch, Phys. Lett. 87B, 193 (1979).
- ¹⁰F. G. Perey (unpublished); B. S. Nilsson (unpublished).
- ¹¹L. Meyer, Phys. Status Solidi 44B, 253 (1971).
- ¹²J. Gomez Del Campo and R. G. Stokstad (unpublished).
- ¹³J. J. Kolata, R. M. Freeman, F. Haas, B. Heusch, and A. Gallmann, Phys. Rev. C 19, 408 (1979).
- ¹⁴J. J. Kolata, R. M. Freeman, F. Haas, B. Heusch, and A. Gallmann, Phys. Rev. C 19, 2237 (1979).
- ¹⁵F. Pühlhofer, Nucl. Phys. A280, 267 (1977).
- ¹⁶B. Kohlmeier, W. Pfeffer, and F. Pühlhofer, Nucl. Phys. A292, 288 (1977).
- ¹⁷B. Heusch, C. Beck, J. P. Coffin, R. M. Freeman, A. Gallmann, F. Haas, F. Rami, P. Wagner, and D. E. Alburger, J. Phys. (to be published).
- ¹⁸A. Weidinger, F. Busch, G. Gaul, W. Trautmann, and W. Zipper, Nucl. Phys. A263, 511 (1976).
- ¹⁹T. M. Cormier, J. Applegate, G. M. Berkowitz, P. Braun-Munzinger, P. M. Cormier, J. W. Harris, C. M. Jachcinski, and L. L. Lee, Jr., Phys. Rev. Lett. 38, 940 (1977).
- ²⁰Y. Abe and F. Haas (unpublished).
- ²¹F. Haas, in Deuxième Colloque Franco-Japonais de Physique Nucléaire avec des Ions Lourds, Gif-sur-Yvette, 1979, edited by the Commissariat à l'Energie Atomique, Saclay, France, 1980, Report No. ISBN-2-7272-0048-X.